

Plasma dynamics in counter-facing plasma-focus type extreme-ultraviolet light source

Kenta Kawaguchi, Tatsuya Sodekoda*, Hajime Kuwabara*, Masashi Masuda, Shi Jia Liu, Kouki Kanou, Mitsuo Nakajima, Tohru Kawamura, Kazuhiko Horioka

Department of Energy Sciences, Tokyo Institute of Technology, Yokohama 226-8502, Japan

**Research Laboratory, IHI Corporation, Shin-nakaharacho 1, Isogo-ku, Yokohama 235-8501, Japan*

ABSTRACT

We have developed a counter-facing plasma focus device for the next generation Li plasma light source of photo-lithography. The plasma dynamics in counter-facing plasma focus was discussed to optimize the operating condition. We obtained time-resolved spectra of the Li-plasma, which showed spectral purity evolves as a function of time. Based on the results, we estimated a current sheet profile and the total amount of Li mass that contributes the focusing plasma.

Keywords

EUV lithography, Plasma focus, Lithium emission, Spectroscopy, Plasma diagnosis

1. Introduction

Extreme-ultraviolet (EUV) lithography is eager to put it into practical use. For the practical application, we have to develop an efficient light source in wave-length region of $13.5\text{nm} \pm 1\%$ (in band).

A properly controlled plasma composed of hydrogenlike Li has a strong line emission at 13.5 nm. Compared with other plasma source, it has some advantages for EUV light source such as little heating load from out-of-band emissions and less energetic debris [1]. To get a lot of 13.5 nm photon fluence, we have developed a new type of DPF type device [2, 3].

Figure 1 shows emissivity of the Lyman- α line originated in hydrogen-like Li ions. We used a collisional-radiative rate equation model for the calculation [4]. In the calculation, we assumed pure Li-plasma and neglected the effect of doubly excited states.

An expected spectral efficiency of in-band emissions ($13.5\text{ nm} \pm 1\%$) is shown in Fig. 2. In the calculation [5], emissivity of the Li plasma was estimated in a range from 9.5 nm to 124.0 nm.

As we see in Fig. 1 and Fig. 2, there are optimum

operating conditions for the emissivity and the spectral efficiency. This means the purity and intensity of the line emission are provided basically by the plasma temperature and density which are determined by the plasma dynamics. If we can confine the plasma for more than μs , the high energy density plasma may realize an efficient and high average power EUV source [6]. In order to optimize the operating condition, it is important to know the Li plasma dynamics in the counter-facing plasma focus.

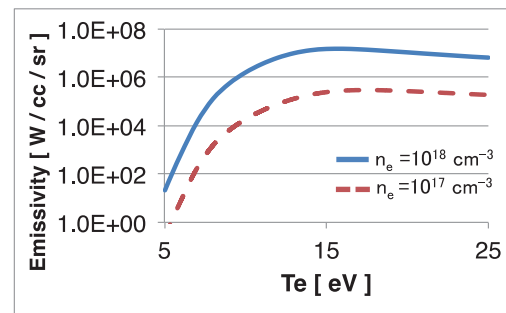


Fig. 1 In-band-emissivity of lithium Lyman- α line ($13.5\text{ nm} \pm 1\%$) vs. electron temperature T_e .

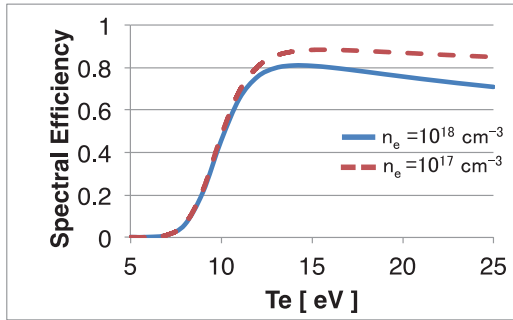


Fig. 2 Estimated spectral efficiency of Li-plasma as a function of electron temperature. Spectral efficiency of $13.5 \text{ nm} \pm 1\%$ was calculated by integration of pure Li emissivity from 9.5 nm to 124.0 nm .

To know the plasma behavior, we tried time-resolved EUV optical emission spectroscopy (EUVOES) for the counter-facing plasma focus. From the evolution of spectra, we could estimate the amount of Li plasma and understand some plasma dynamics.

2. Experimental Setup

Figure 3 shows a schematic illustration of the counter-facing plasma focus device and the EUV

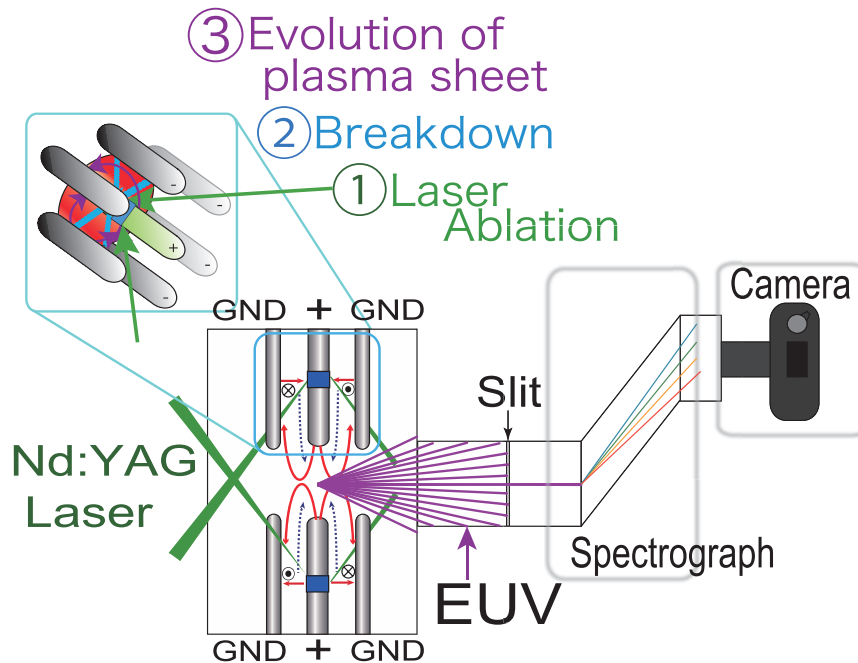


Fig. 3 Schematic of the discharging device and the EUV spectrograph by using diffraction grating plate and MCP controlled by driver circuit.

spectrometer composed of a diffraction grating (HITACHI-No.001-0437) and a MCP (F2223-21P) which is controlled by a gate-driver circuit. The image of the MCP was recorded by a CCD camera. Figure 4 shows typical geometry of the focus electrodes.

First, initial plasma is made by Nd-YAG laser from solid Li at the root of the inner electrodes. The laser energy is about 20 mJ/beam/15ns . Second, a discharge between the inner and outer electrodes is triggered by the laser ablation. Third, the plasma sheet is accelerated in the direction of the center of the gap between the counter-facing electrodes. And then, the plasma begins to pinch, be thermalized, and emits the light in EUV region.

This spectrograph has sensitivity in a range from 12 nm to 30 nm . When the focus device was in operation, a high voltage from $+5 \text{ kV}$ to $+7 \text{ kV}$ was applied between the inner and outer electrodes, and a discharge was driven by 6 capacitors of $2.4 \mu\text{F}$ in total.

As shown in Fig. 3, there are 6 outer electrodes which have inductively isolated current paths.

The EUV spectrograph has temporal resolution of 200 ns with the fast gate driver using MOSFET.

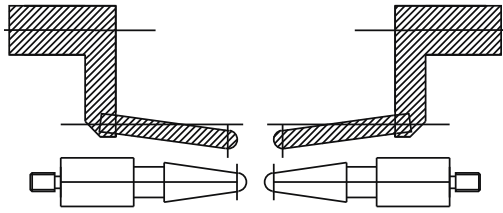


Fig. 4 Geometry of the electrodes

3. Results and Discussion

3.1 Characteristics of plasma focus phenomena

A time-integrated photograph of the plasma in the counter facing plasma focus device is shown in Fig. 5, where the device was operated with positive-positive mode. As we can see in Fig. 5, the pinch plasma was formed at the center of two electrodes. Strong green light at the roots of the electrodes was caused by the scattering of Nd-YAG (2ω) laser.

Figure 6 shows typical spectrum image of the EUV plasma. By converting the information on the pixels of the CCD camera into wavelength, we can obtain the spectrum intensity vs. wavelength.

Figure 7 shows typical discharge current profiles at the inner electrode, for operations with single focus mode and the counter-focusing mode. Here, $t = 0$ is defined at the laser trigger signal.

3.2 Results and Discussions

There was a difference in the current periods between counter-facing plasma focus and single plasma focus (see Fig.7). From a LCR circuit equation, we estimated that a difference of $0.2\mu\text{s}$ current period is caused by a difference of 2nH inductance of current path. The difference of inductance can be attributed to the evolution of plasma sheet. Figure 8 shows the evolution model of the current sheet in the single plasma focus mode.

On the other hand, Fig. 9 shows the expected current sheet behavior in the counter-facing plasma focus device.

As we show in Fig. 8 and in Fig. 9, the protrusion of current sheet in the counter-facing plasma focus seems to be suppressed. Therefore, a current period of the counter facing plasma focus becomes shorter

than that of the single plasma focus because of smaller inductance.

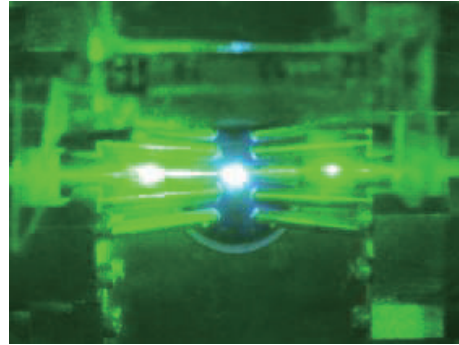


Fig.5 Time-integrated photograph of the plasma in counter-facing plasma focus.

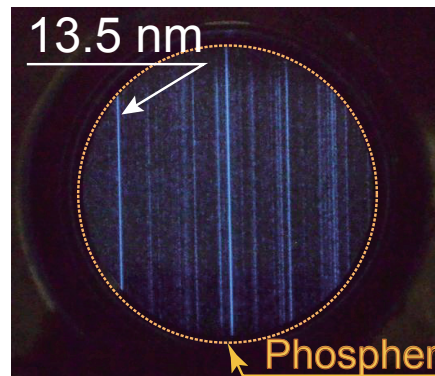


Fig. 6 Typical spectrum of Li plasma.

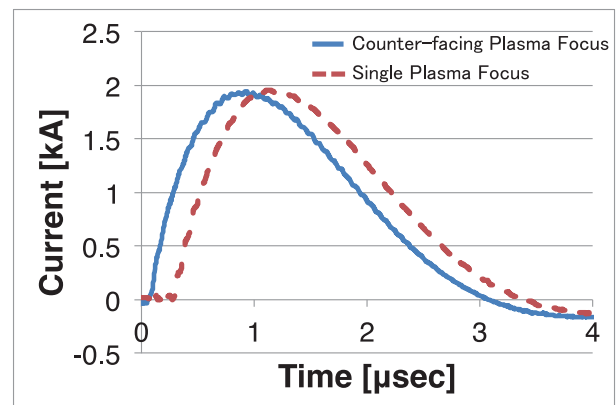


Fig.7 Typical current profiles. Solid line shows the current in counter facing plasma focus device and dotted line shows that in single plasma focus mode.

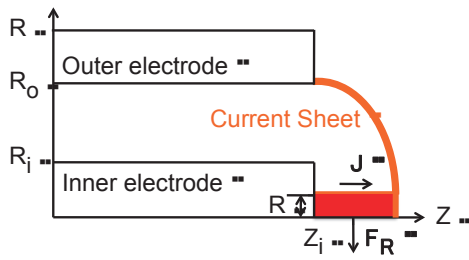


Fig. 8 Evolution of current sheet in single plasma focus mode.

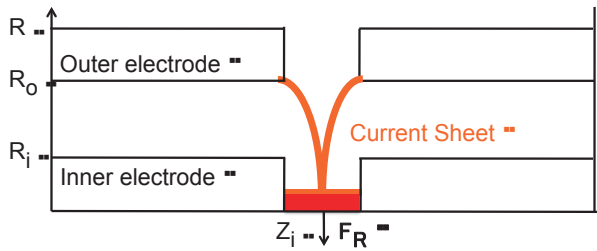
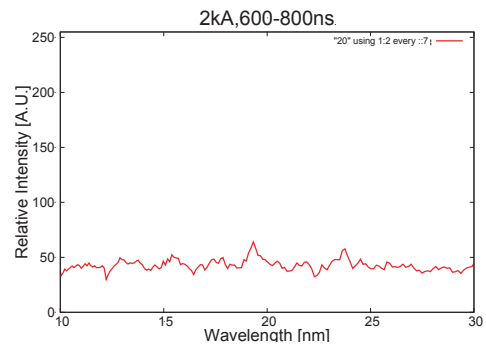


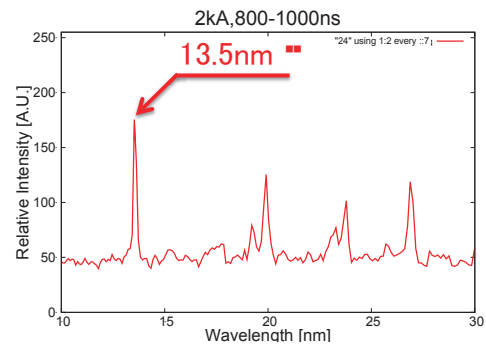
Fig. 9 Expected evolution of current sheet in counter-facing plasma focus device.

Figure 10 (a) - (e) show the results of time-resolved EUV optical emission spectroscopy. As shown in Fig. 10 (b), the 13.5nm line emission appears 800-1000ns after the laser trigger and that evolves to continuous spectra around 1800ns. This result suggests that the best condition for EUV light source is the beginning of the EUV emission from the point view of spectrum purity. At this moment, Li plasma may be strongly confined by the counter-facing current sheet and hold the temperature of electrons, at least, over 10eV.

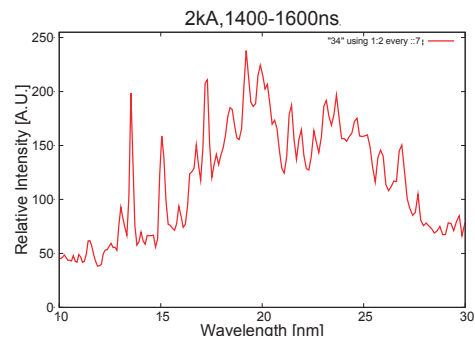
As time goes by, the constraint force of self magnetic field seems to become insufficient to confine the plasma. Hence the plasma starts to diffuse and emit various spectral lines. Figure 10 revealed that the in-band EUV emission was maintained for $\sim 1\mu s$, which is almost 10 times longer than those of conventional plasma EUV light sources.



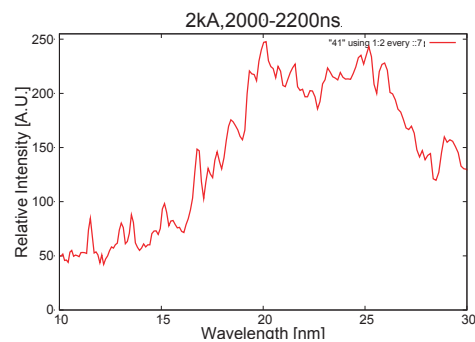
(a) t = 600-800 ns



(b) t = 800-1000 ns



(d) t = 1400-1600 ns



(e) t = 2000-2200 ns

Fig.10 Time-evolution of EUV spectra from counter-facing plasma.

Assuming 1-D equation of motion driven by electro-magnetic force and the plasma mass is constant, the displacement of the plasma z can be described by the equation below,

$$z = \iint \frac{1}{M_z} \frac{\mu_0}{4\pi} \ln\left(\frac{R_o}{R_i}\right) I^2 dt dt \quad (1)$$

where M_z is the mass of plasma; μ_0 is the permeability; R_i and R_o are the radii of the inner and outer electrodes; and I is the single channel current through the plasma.

Figure 11 shows the plasma axial displacement estimated by the dynamics model of plasma focus and measured current profile I . As shown, the plasma arrives the center of gap between two electrodes, at least 800ns after the laser triggering (see Fig. 10). The distance between the laser spot and the center gap between two electrodes was about 18mm. So we can estimate the mass of the plasma which is confined is $\sim 1.0\text{ng}$ for each current path. Therefore the total mass of the confined plasma was estimated to be $\sim 12\text{ng}$ because the discharge plasma is driven by 12 channels.

If the plasma is closed in a sphere having 3mm diameter, the density of plasma is estimated to be $\sim 10^{17}\text{cm}^{-3}$, which is the best density from the view of spectral efficiency as shown in Fig.2.

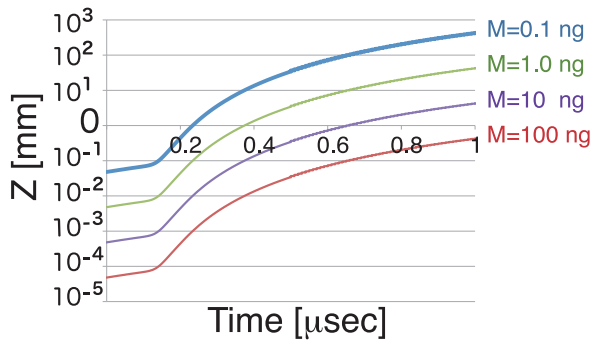


Fig. 11 Plasma axial displacement z estimated using 1-D dynamics model of plasma focus and measured current profile.

4. Concluding Remarks

We studied the plasma dynamics in the counter-facing plasma focus device. We got the current data and the time-resolved EUV OES data. We discussed the correlation between the plasma dynamics and the experimental results. Two issues were clarified from the results. One is the evolutions of the current sheet profile in the focus device. Another is the estimation of the amount of plasma closed in the center of gap between two electrodes. That is, the amount of plasma contributing the EUV emission.

What we should do next is estimating the evolution of electron temperature because we can know more detailed plasma dynamics if we do this. By that means, we can optimize the operating condition of the counter-facing device.

References

- [1] Coons RW, Harilal SS, Campos D, Hassanein A, "Analysis of atomic and ion debris features of laser-produced Sn and Li plasmas", J Appl Phys 108(6):063306(2010).
- [2] Y. Kuroda, K. Hayashi, H. Kuwabara, M. Nakajima, T. Kawamura, and K. Horioka. "Counter-facing plasma guns for efficient extreme ultra-violet plasma light source". In NIFS-PROC-90, (2012).
- [3] H. Kuwabara, K. Hayashi, Y. Kuroda, H. Nose, K. Hotozuka, M. Nakajima, K. Horioka, "Counter-facing plasma focus system as an efficient and long-pulse EUV light source", Proc. SPIE 7969 (2011).
- [4] T. Ozawa, S. Yamamura, N. Tatsumura, K. Horioka, and T. Kawamura, "Lasing of extreme ultraviolet light with nitrogen plasma in a recombining phase-Roles of doubly excited states", Phys. Plasmas **19**, 063302 (2012).
- [5] T. Kawamura, K. Mima, F. Koike, "Line shapes of He beta including higher-order satellite lines for Ar ions in dense plasmas", Plasma Phys. Controlled Fusion **43**, 53 (2001).
- [6] M. Masnavi, M. Nakajima, E. Hotta, K. Horioka, Appl, Phys.Lett., 89, 031503 (2006)